Environment and Planning B: Planning and Design 2008, volume 35, pages 413 – 430

doi:10.1068/b33075

Modeling cities in 3D: a cellular automaton approach

Lucien Benguigui
Solid State Institute and Physics Department, Technion – Israel Institute of Technology, 32000 Haifa, Israel; e-mail: ssgilles@tx.technion.ac.il

Daniel Czamanski ¶, Rafael Roth
Complex City Research Lab, Faculty of Architecture and Town Planning, Technion – Israel Institute of Technology, 32000 Haifa, Israel; e-mail: danny@czamanski.com, rothr@tx.technion.ac.il
Received 9 June 2006; in revised form 23 January 2007; published online 26 March 2008

Abstract. This paper presents a quasi-3D cellular automaton (CA) simulation model of cities. A 2D CA model includes a cell attribute that represents building height information. Dynamic processes are depicted using four parameters: initial building coverage, interaction with adjacent neighborhood, inertia, and noise. These parameters can assume simple economic interpretation. Some combinations of values of the parameters result in cities that experience paths of convergent growth. Some values lead to cities that experience phase transitions. We suggest a typology of resulting urban patterns and note the emergence of spatial clusters of high-rise buildings.

1 Introduction

The temporal and spatial evolution of urban spatial structures has been the subject of research for quite a few years now. Urban spatial dynamics are discontinuous in space and nonuniform in time. As a result, precise descriptions are elusive. In a series of previous papers we depicted, analyzed, and provided at least partial explanations of the spatial complexity of Tel Aviv (Benguigui et al, 2000; 2001a; 2001b; 2006). However, all past work was based exclusively on historic 2D data of urban footprints and on socioeconomic time series and cross-section data representing administrative jurisdictions.

Cities, however, are 3D objects. It is to be expected that the footprints of cities capture only partly the nature of the dynamics of urban morphology. The objective of this paper is to explore a cellular automaton (CA) simulation model of a 3D city. The simulations were carried out using StarLogo software. It depicts 3D urban dynamics on a 2D grid with the height attribute of the cells as the third dimension.

Section 2 presents a short survey of urban and dynamic simulation models. Despite the multiplicity of cellular models of urban spatial sprawl, there is a paucity of 3D models. Sections 3 and 4 include detailed description of the model and preliminary simulation results that illustrate the characteristics of the model. Section 5 presents some examples of real cities. Conclusions are presented in section 6.

2 Past work

From the early years of the 20th century, the study of cities, and in particular of urban growth, has attracted researchers from a variety of disciplines. Urban growth has been studied with tools from geography (Krakover, 1985), economics (Fujita et al, 1999) and synergetics (Portugali, 2000). In addition to analytic models, insights have been sought by means of computer simulations and by means of concepts such as fractals and percolation.

¶ Corresponding author.

Traditional urban models were concerned with the reasons for spatial agglomeration of people and of activities, the formation of cities and with the dispersion of people and activities within cities from their centers outwards towards urban peripheries (Glaeser and Kahn, 2001). The dominant approach visualizes the growth of cities as a sand pile of people and of activities that grows from its pinnacle at the center outwards. As more people and activities are added the center increases in volume. As a result of competition many are pushed away from the center and the periphery, much less dense, expands outwards (Alonso, 1964). A stylized moving wave, or front of expansion, is envisaged.

This traditional view of urban expansion was a useful framework for formulating basic models of urban spatial behavior and it did yield a number of very interesting insights. A somewhat more sophisticated approach took into account that the old central business districts are accompanied by secondary centers, generally at the cities' edges (Garreau, 1992; Krugman, 1996). Theoretical models focused on the examination of equilibrium conditions for the common polycentric urban structures (Fujita, 1982; 1990; Henderson, 1974). Empirical work attempted to identify subcenters (McMillen and Smith, 2003). These newer analyses are also rather imprecise descriptions of the urban reality.

There have been very few attempts to study cities as 3D dynamic objects. Cellular automata models are a useful tool for analyzing discrete spatiotemporal dynamics of cities in two dimensions (Batty, 1998; 2005; Cheng and Masser, 2004; Couclelis, 1997; White and Engelen, 1997). They were originally developed in the context of other disciplines (Wolfram, 1986) in which 3D models were developed (Hua and Sprung, 1998; Hunt et al, 2005; Siregar et al, 1998). The pioneering work of Semboloni in simulating the evolution of virtual cities (Semboloni, 1997; 2000a; 2000b) suggests that the 3D growth of cities results in spatial specialization in terms of types of land uses. The appearance of mixed land uses is rare. In Semboloni's models the weight of the neighboring land uses in the development potential function for a given site dominates land uses that do not already exist on the site. Another interesting result in Semboloni's model is that the height of buildings declines in concentric circles around some urban center.

These are the familiar results of traditional monocentric urban models displaying declining rent gradient. However, at best these results are an imprecise depiction of urban morphology.

3 3D cellular automaton simulation model of urban sprawl

In this paper we present a 3D CA simulation model in which the city's shape is referenced by means of temporal changes in the volume of buildings, the height distribution of buildings, and their spatial distribution.

On the basis of past 2D simulation work, we demonstrate that it is possible to generate a description of the 3D development of cities. It is our expectation that, given the performance of our model, it will be possible to expand the 2D results into a more realistic 3D context. Even though our results are preliminary, they suggest that:

(1) It is possible to generate a 3D urban morphology that approximates a real city by means of a CA simulation model.

(2) The simulated 3D distribution of buildings is discontinuous in space and nonuniform in time. The main components of an urban morphology are 3D clusters; clusters are defined as spatially continuous concentrations of buildings of predefined heights that can be quantified.

(3) 3D urban morphology can be represented by leapfrogging processes (see Benguigui et al, 2001b). The development of 3D clusters starts at a specific location, proceeds in a continuous fashion from that location outward and after some time leaps spatially to a new location.
(4) Percolation is present in the simulated 3D morphology.

Behind our model there is the well-established conception that cities are spatial self-organizing systems. The observed spatial macro order is the result of a dynamic process of self-organization that originates in forces that are internal to the system. The CA simulation represents a simple representation of a self-organizing system.

In our model the evolution of a city's height is represented by a development potential function which is a function of four parameters representing four simple economic factors: initial coverage, inertia factor, interaction factor, and a noise factor. However, unlike in aforementioned models (Batty, 1998; Semboloni, 1997; White and Engelen, 1997), our development potential is a Boolean discrete function and not a continuous function.

We introduced a simple set of Boolean decision rules with variables that take on the values 0 or 1 for each cell and at all times. The development potential function receives a value of 0 for a cell if no building activity will take place in the given cell at a given time; a value of 1 indicates that the building on the given site will be replaced by a higher building in the coming period. The parameters that govern the decision rules concerning all cells can be preset for the entire run of the model, they can be changed in the midst of a run based on preselected conditions, or they can change randomly. The values of global parameters (initial coverage, inertia, and noise) are between 0% and 100%, which represent their intensity. The parameters are:
(1) initial coverage—this represents the preliminary building share of the surface. The initial height of buildings is Δh (in floor units).
(2) inertia—this factor represents the notion that the building process in a given geographic neighborhood has a continuous and self-reinforcing dynamic. A cell that was built up in a given period will continue to be built with a predetermined probability in the next period.
(3) interaction—this is a threshold parameter and it is defined as the sensitivity of a cell to the building activities in its neighborhood. Its range of values is between 0 and N (which is the number of cells in the nearest neighborhood).[1] This factor represents the well-known agglomeration effect externality and its direct impact on the desire to capitalize through appropriate building decisions.
(4) noise – this is a purely random factor that accounts for all the influences not captured by the above factors. The values 0 and 1 are assigned randomly according to this parameter. The noise factor is the uncontrolled component of the decision rule. It is assumed to be uncorrelated with the other factors and processes.

Every cell in the surface is located at coordinates (x, y) on the grid and has its own values of interaction, inertia, and noise. The model's parameters (initial coverage, inertia, interaction, and noise) can be controlled and their values are global to the entire surface.

The inertia characteristic I of location (x, y) at time t is depicted in expression (1):

$$\mathrm{I}(x, y, t) = \begin{cases} 1, & \text{if} \quad \Delta\,\text{height}\,(x, y, t-1) = \Delta h, \quad \text{with probability inertia}, \\ 0, & \text{if} \quad \Delta\,\text{height}\,(x, y, t-1) = 0; \end{cases} \tag{1}$$

[1] The size and type of neighborhood has a crucial effect on the simulation's results (Chen and Mynett, 2003; Kocabas and Dragicevic, 2006). In this study we propose the use of the Moore neighborhood, which consists of all eight surrounding cells, because spatial influences and forces on land parcels are potentially created from all nearest parcels around.

where

$$\mathrm{I}(x,\ y,\ 0) \ = \ \begin{cases} 1, & \text{with probability } \textsf{initial coverage}\,, \\ 0, & \text{with probability } 1 - \textsf{initial coverage}\,; \end{cases}$$

In other words, the inertia of location (x, y) at time t is a function of the change in height in this location over the previous period $[\Delta\text{height}(x, y, t-1)]$. If there was change of Δh floors (5 floors in our simulations), the inertia receives the value '1' with a given probability according to the global parameter inertia and otherwise it gets a value '0'.

The interaction parameter has a threshold between 0 and 8 cells, and it represents the minimum number of growing adjacent cells required for the interaction of location (x, y) to become '1'. The interaction characteristic S of a specific location is depicted in expression (2):

$$\mathrm{S}(x,\ y,\ t) = \begin{cases} 1, \text{ if } \displaystyle\sum_{\forall (x',\ y') \in \Omega} \mathrm{P}(x', y', t-1) \geqslant \textsf{interaction},\ 0 \leqslant \textsf{interaction} \leqslant 8(\text{cells}), \\ 0, \text{ if } \displaystyle\sum_{\forall (x',\ y') \in \Omega} \mathrm{P}(x', y', t-1) < \textsf{interaction},\ 0 \leqslant \textsf{interaction} \leqslant 8(\text{cells}); \end{cases} \tag{2}$$

In words, the catalyst for the aggregation of height changes is to be found at the previous time in the adjacent cells. Adjacent cells are located in the 'Moore neighborhood' (eight surrounding cells)—indicated by the Ω symbol. If the sum of 'potential' P in the neighborhood is greater than the global threshold, the interaction of a cell receives a value of '1'.[2] The potential development function of a cell in location (x, y) at a time t is a Boolean variable, which has only two values: '1' represents a decision to build an additional Δh floors at time t, and '0' represents the status quo at that location.

The noise value of location (x, y) at time t is '1' with probability noise, and its value is '0' with the complement probability. It has the following expression:

$$\mathrm{N}(x,\ y,\ t) \ = \ \begin{cases} 1, & \text{with probability} \quad \textsf{noise}\,, \\ 0, & \text{with probability} \quad 1 - \textsf{noise}\,; \end{cases} \tag{3}$$

The city building process proceeds at a pace of Δh floors. A decision to build in a particular cell results in an addition of Δh floors in a given period. The decision to build depends on at least two out of the three factors receiving a value '1'. Table 1 presents the truth values of the potential to build for every location (x, y) at time t. As can be seen from this table, only a combination of at least two variables with value '1' can trigger a decision to build Δh more floors at that location.

Table 1. The 'truth table' of the potential function of location (x, y) at time t. A combination of at least two variables with value '1' can lead to building activity. $\mathrm{S}(x, y, t)$, $\mathrm{I}(x, y, t)$, $\mathrm{N}(x, y, t)$, and $\mathrm{P}(x, y, t)$ denote interaction, inertia, noise, and potential, respectively.

$\mathrm{S}(x, y, t)$	$\mathrm{I}(x, y, t)$	$\mathrm{N}(x, y, t)$	$\mathrm{P}(x, y, t)$	Build?
0	0	0	0	no
0	0	1	0	no
0	1	0	0	no
0	1	1	1	yes
1	0	0	0	no
1	0	1	1	yes
1	1	0	1	yes
1	1	1	1	yes

(2) The simulation model has one more possible version of interaction parameter, which represents the threshold in terms of the average of adjacent heights.

The dynamics of the heights H in the model can be expressed as follows:

$$\mathrm{H}(x,\ y,\ t) \;=\; \mathrm{H}(x,\ y,\ t-1) + \Delta h \mathrm{P}(x,\ y,\ t-1)\ , \tag{4}$$

subject to $\mathrm{H}(x,\ y,\ t) \leqslant H_{\max}$; and $\mathrm{t} \leqslant \mathrm{T}$.

According to this expression, new buildings, which are Δh floors higher, can be established instead of the old one. $H_{\max}$ is the height limitation in the simulations and T is the user-controlled number of periods in the running of the model. It indicates the last period during which a change in height occurred. This is the period during which the model reaches its steady state and a convergence path. Steady state in the simulation model describes the spatial order at the end of the transition process. The model also enables the representation and analysis of non-steady-state spatial patterns, which are outside equilibrium.

4 Simulation results

The 3D model was implemented by means of the StarLogo software (2006) developed at MIT and customized for this particular study (see figure 1). It simulates 3D evolution of a city on a 2D square base. A cell can represent a single building, a city block, or an entire neighborhood. It represents a site ripe for building activity. Building height is measured in terms of the number of floors. This number is a variable associated with each cell. The maximum number of floors in this particular model, $H_{\max}$, is 40, but this can be defined differently.

This chapter is divided into three parts. Section 4.1 deals with static or steady state spatial order, section 4.2 deals with dynamic processes and transitions, and section 4.3 presents histograms of heights in the simulated cities.

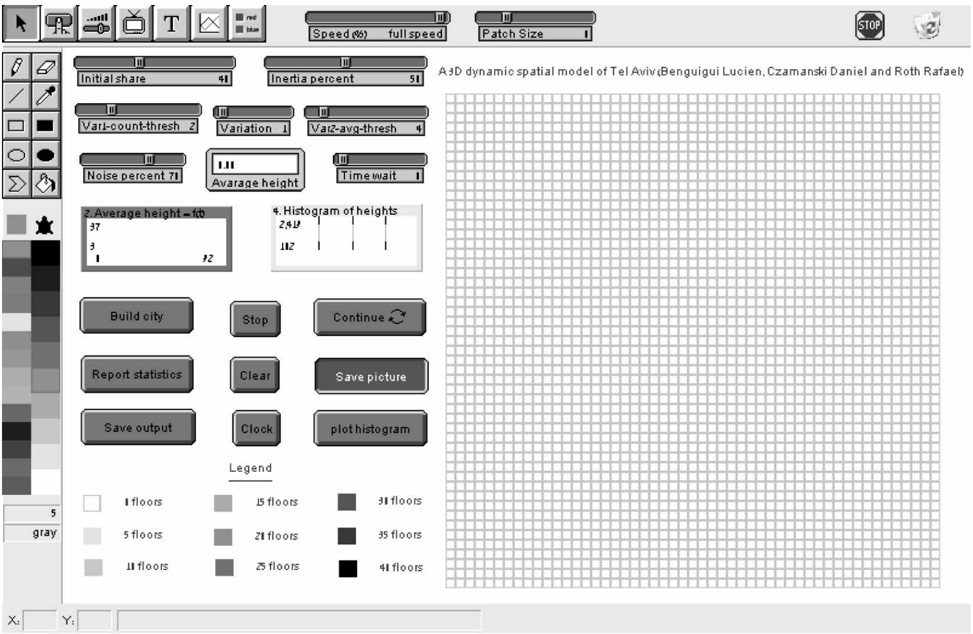

Figure 1. User interface of the CA simulation model—parameters can be adjusted by sliders and the dynamics represented on a 2D grid surface.

4.1 Static results

It is very clear from the first applications of our 3D CA simulation model that it is possible to generate a large number of urban morphologies and paths of urban development. Furthermore, various combinations of user-controlled parameters can result in stable and converging distributions of building heights. Thus, for example, high values for the parameters initial coverage, inertia, and noise, and a low value of interaction, result in an ever-growing city with divergent average height. Figure 2 presents one example of the tests. There is a clearly defined border between convergence and divergence regions and it depends on parameter values. The border mapping was conducted for constant values of the parameters initial coverage and inertia (40% and 100%, respectively, in the specific example).

Numerous simulations produced cities with different shapes in steady state. We can identify five types of city pattern:

(1) *Class a* cities—very low and flat cities, without a significant development of skyscrapers or high buildings. This class can represent a city in its early development stages from a flat city with low average height to a modern and high city in further generations of development. Figure 3 illustrates class a cities. Cities in this class can be

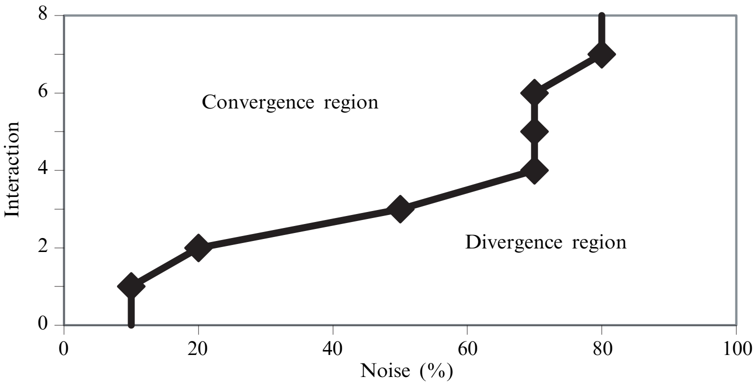

Figure 2. Convergence and divergence regions in the model for initial convergence = 40% and inertia = 100%. There is a clear boundary between the regions.

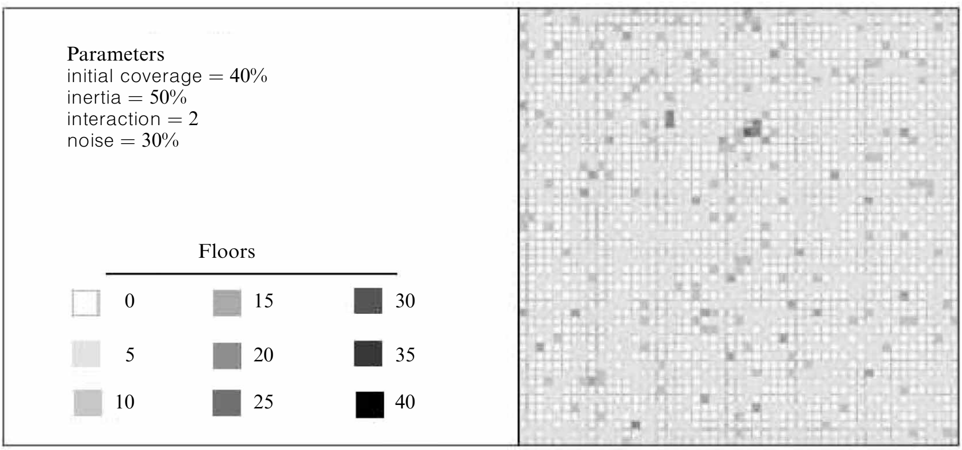

Figure 3. Class a cities with low buildings, where inertia and noise have low values (50% and 30%, respectively).

produced by small values of the inertia and noise parameters and a high value of the interaction parameters.

(2) *Class b* cities—these cities have a few high buildings, but those towers are separate entities without any significant agglomerations, or spatial clusters. Cities in this category can be in a transition process from class a to class c, but they can stay in this category at a steady state. Figure 4 illustrates class b cities. These cities are produced by a high value of the inertia parameter, which indicates strong reinforcing forces, and a high value of the interaction parameter, which indicates a weak influence from the adjacent neighborhood.

(3) *Class c* cities—in this case there are separate clusters of high buildings. The agglomerations can be thin or thick, but there is no connection between them. This class represents modern cities with agglomerations of towers. The land uses in the clusters are often homogeneous, just like retail agglomerations, resident clusters, or hotel areas. Many cities belong to this class. Figure 5 illustrates class c cities. The towers are gathered in separate agglomerations. The location of clusters is random, but there is spatial order reminiscent of a real large city.

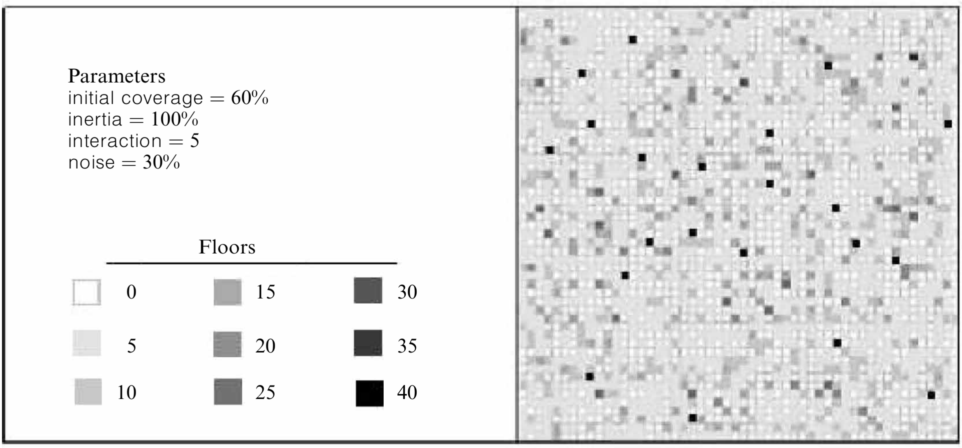

Figure 4. Class b cities with separate high towers, where inertia has a high value (100%) and interaction is high (5).

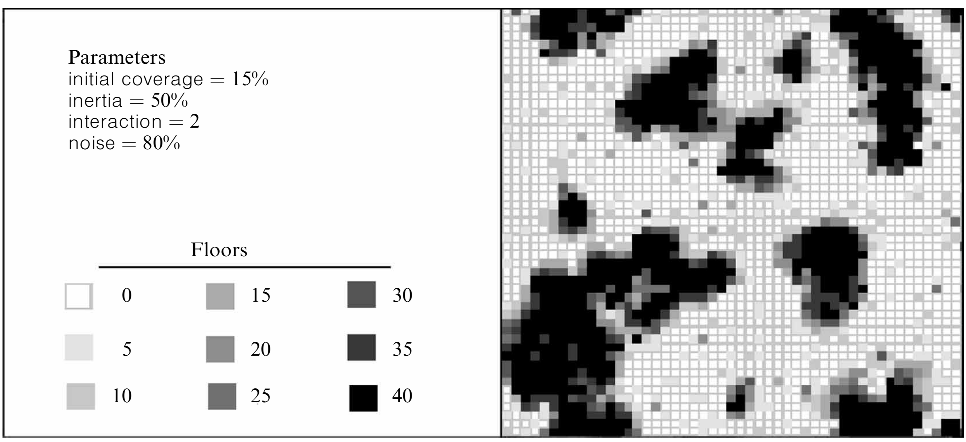

Figure 5. Class c cities with spatial clusters of towers—interaction, and inertia have low values (2 and 50%, respectively).

(4) *Class d* cities—here the spatial clusters are interconnected and form long chains. Such cities illustrate the phenomenon of full percolation of the surface. Figure 6 is an illustration of class d cities. These cities have spatial clusters similar to class c cities, but in the case of class d the clusters are merged together and generate long chains of high buildings. In this context it is noteworthy that in real cities there are also wide regions of medium-sized buildings that coexist with the pattern of class d cities. Furthermore, class d cities illustrate the phenomenon of full percolation. The ranges of parameters that can generate class d cities are not unique, but they result from high values of the inertia and noise parameters and low values of the interaction parameter.
(5) *Class e* cities—this class represents virtual cities on a divergence course. These cities grow forever without limitation. Figure 7 illustrates class e cities. This spatial order represents a divergent path of growth. The present model can generate extreme outcomes like this by using very high values of inertia and noise, and a very low value of interaction.

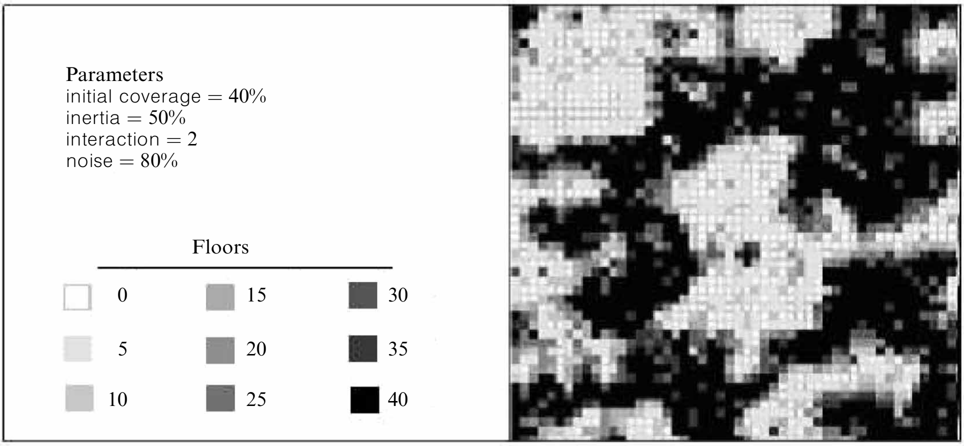

Figure 6. Class d cities with connected chains of clusters, where interaction and inertia values are low (2 and 50%, respectively) and noise value is very high (80%). This figure illustrates the phenomenon of full percolation of the surface.

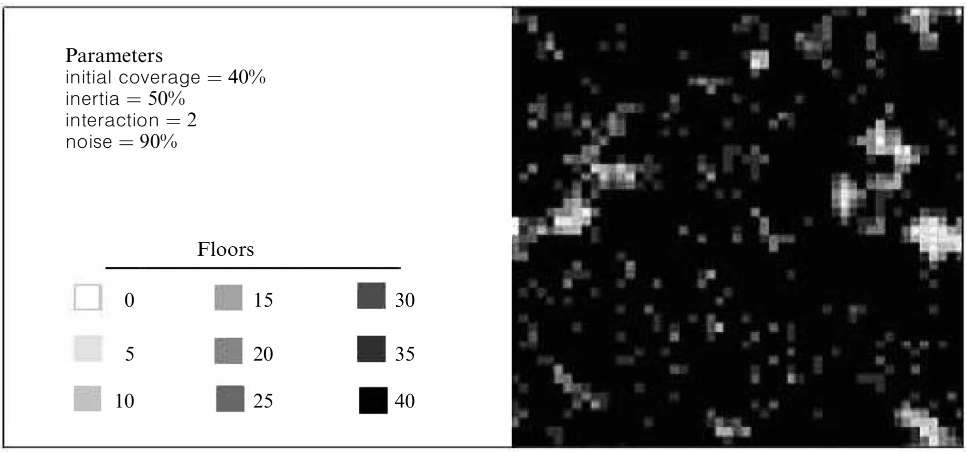

Figure 7. Class e cities with a divergent path of growth of very high buildings, where interaction is low (2) and noise value is very high (90%).

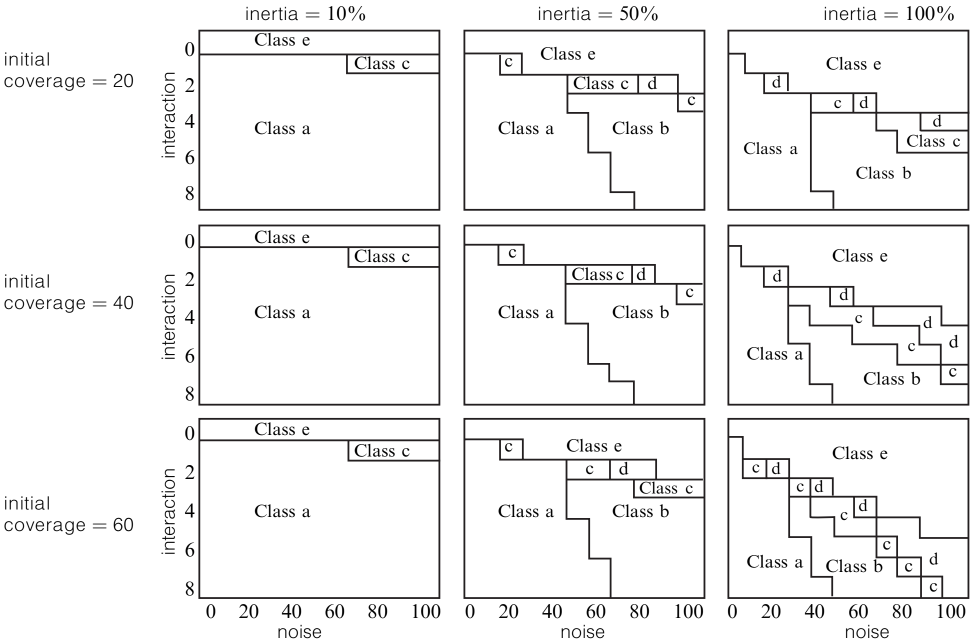

Figure 8. Map of the ranges of parameters—the letters (a, b, c, d, e) represent the different classes as a function of parameter values.

As figures 3 – 7 illustrate, the model generates five distinct spatial patterns (class a – e cities). Systematic variation of the parameter values reveals sharp borderlines between the different patterns. Figure 8 presents a mapping of the various types of cities in relation to parameter values with reference to steady state structures only. In the mapping we set the initial coverage parameter to three alternative values: 20%, 40%, and 60%. The inertia parameter has been set to 10%, 50%, or 100%. The interaction values were between 0 and 8, and the noise varies from 0% to 100% with jumps of 10%. The outputs (city types) are displayed with letters a, b, c, d, and e.

The mapping suggests the following:

- The influence of initial coverage parameter is relatively weak.
- The influence of the three other parameters (inertia, interaction, and noise) is more significant, but we can see strong substitution interdependence between noise and interaction.
- The interaction effect is horizontal (causes the formation of clusters of high buildings, as can be seen in class c cities), and the inertia effect is vertical (causes reinforcing growth, as can be seen in class b cities). The noise effect contributes to the formation of connected clusters (as can be seen in class d and class e cities).
- By changing parameter values with time we can generate cities that experience phase transitions through the distinct classes.

The mapping is a complete static summary analysis of the model. Cities can be developed to various classes in a steady state or as an intermediate stage before equilibrium is reached.

4.2 Dynamic processes

There are several kinds of paths to steady state configurations supported by the simulation model:

(1) *Convergence path with constant parameter values.* At the end of this process the city evolution reaches its final development stage, because parameter values are fixed

through transitions and the city has utilized its development's potential. An example of this converging process is presented in figure 9. The values of parameters are: initial coverage = 15%, inertia = 50%, interaction = 2, and noise = 80%. The final spatial order (class c) is reached after 101 time intervals. The figure presents the change in average height from the initial time to the last period of change.

(2) *Dynamic process with varying values of parameters.* In the initial setup of parameters the city cannot upgrade its spatial pattern, but the parameters can change in time and renew the development. Figure 10 presents the change in average height and we can see a dramatic change in the rate of change after the tuning of parameters. The initial setup of parameters is the same as the previous example (initial coverage = 15%, inertia = 50%, interaction = 2, and noise = 80%), but at time $t = 105$ we have changed the values of inertia to 60% and noise to 100%. The class after 105 intervals is c, with an average height of 5.5 floors, but the final order after many intervals (315 and more) is class e with an average height of about forty floors.

These versions of dynamic processes have to be tested against reality. The important question is can a city change its characteristics in later periods of growth? The model showed that the influence of initial coverage is very weak and even a 'desert land' can develop to a 'skyscraper city'. The important trigger to development is not the initial building share, but the setup of interaction, inertia, and noise parameter values.

Cities can develop to their final stage with different rates of growth. This can be seen clearly by the presentation of average height as a function of time. In its evolution

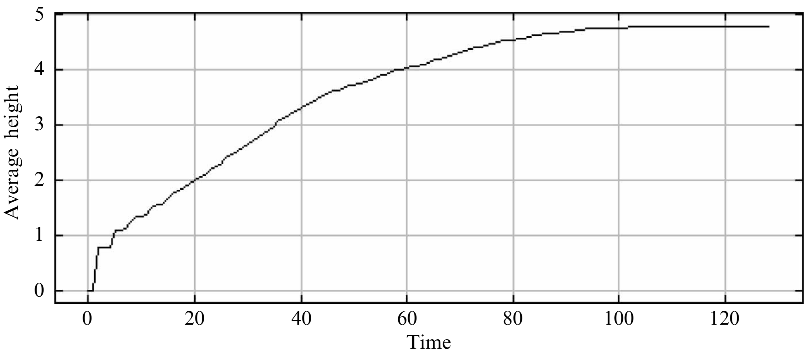

Figure 9. Change in average height from initial time to final steady state, where initial coverage = 15%, inertia = 50%, interaction = 2, and noise = 80%. Steady state is reached after 101 periods.

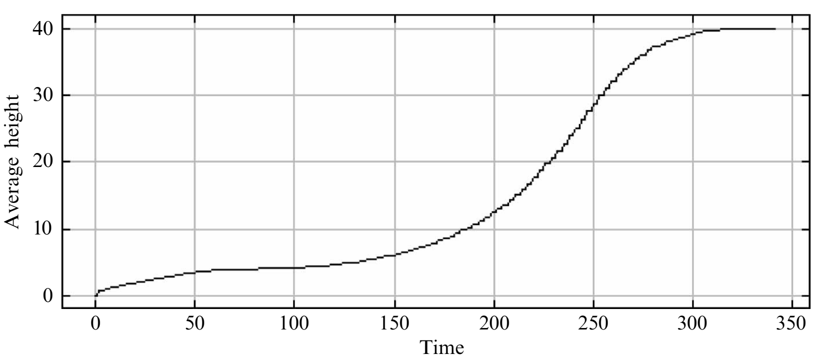

Figure 10. Average height as a function of time, with a change in parameter values after 105 intervals (see text for details). The tuning is of inertia and noise.

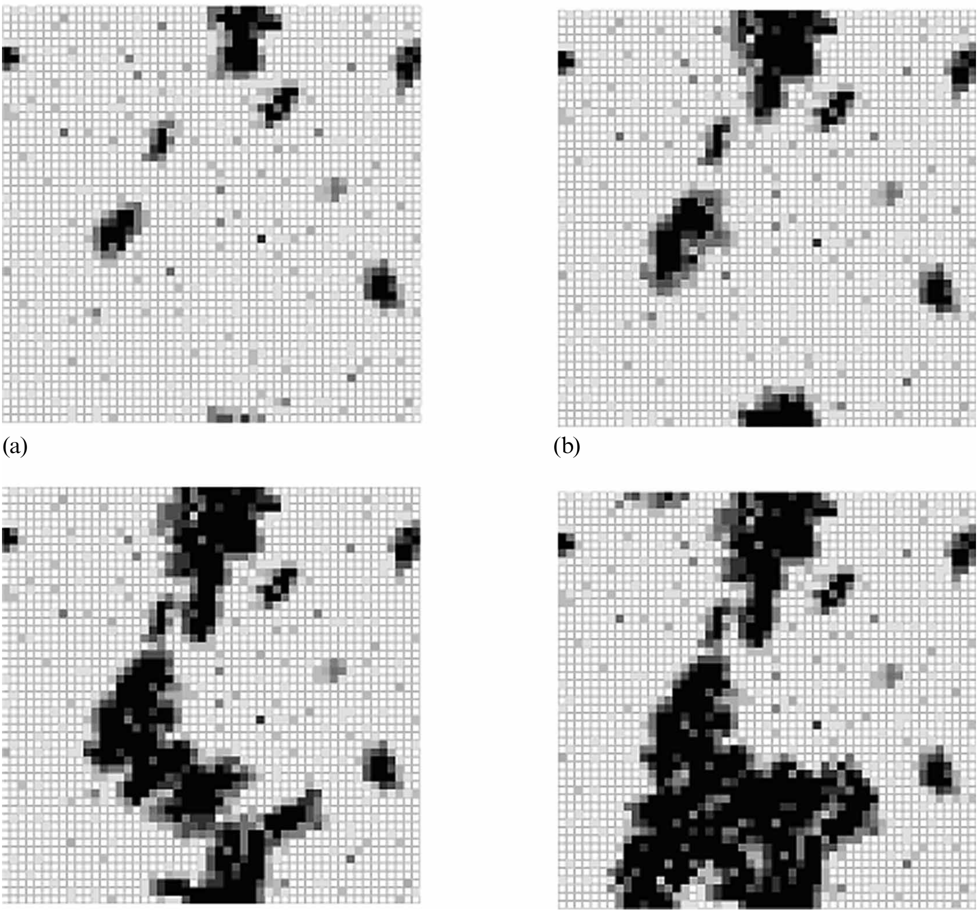

(a) (b) (c) (d)

Figure 11. Illustrations of possible spatial transitions through different classes: (a) after 15 periods; (b) after 25 periods; (c) after 60 periods; (d) after 100 periods and more. The city is of class c after 15 and 25 periods and of class d after 60 periods or more.

the city can pass through all classes incrementally, or it can leap to advanced classes directly. This depends on the setup of parameters in the model. For example, a city can reach class 'd' by incremental growth through classes a, b, and c, or it can reach class d directly after classes a or b.

It is interesting to consider the spatial process by which cities change and arrive at their steady state. It can be slow or fast and it depends on many variables and influences. The present model does not support a quantitative measure of 'phase transitions'. Figure 11 presents an illustration of the spatial transitions by use of the following values of the parameters: initial coverage = 10%, inertia = 70%, interaction = 2, and noise = 50%. Figure 12(a) illustrates the average height of buildings at each phase of a process with the following values: initial coverage = 40%, inertia = 50%, interaction = 2, and noise = 80%. The vertical bars indicate the specific periods of class transitions, and we can see the change of classes from a to d via b and c. A specific class (like class d in this example) can be reached as a steady state, but it can be only a stage in reaching a steady state, as can be see in figure 12(b). In this run of the model, the values of parameter are initial coverage = 40%, inertia = 50%, interaction = 2, and noise = 90%. Here class d has a different meaning in comparison to the same class in the previous example.

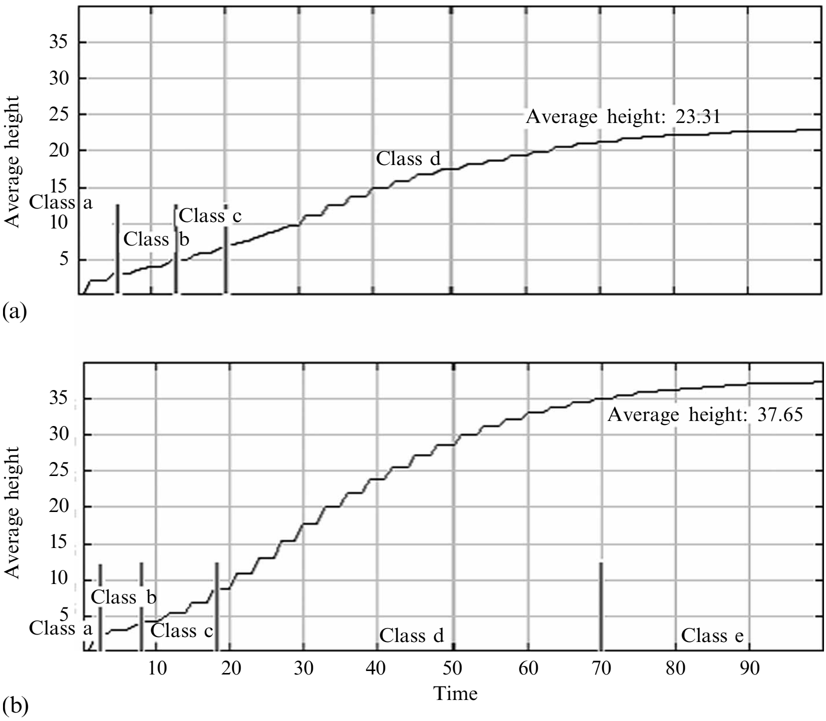

Figure 12. Average height as a function of time (period)—vertical bars indicate the specific periods of class transitions: (a) steady state is reached with class d; (b) steady state is reached with class e.

4.3 Distributions of heights

One more output of the simulation model is the distribution of heights on the square surface. Figure 13 illustrates the distribution of building heights in the class a pattern.(3) As can be seen, the number of low cells (0 or 5 floors) is high (frequencies of 56.9% and 35.7%, respectively), the number of high buildings (35 and 40 floors) is small (frequency of about 0%), and only 7% of the buildings have reached heights which exceed initial heights. The average height in the steady state of this run is 2.6 floors.

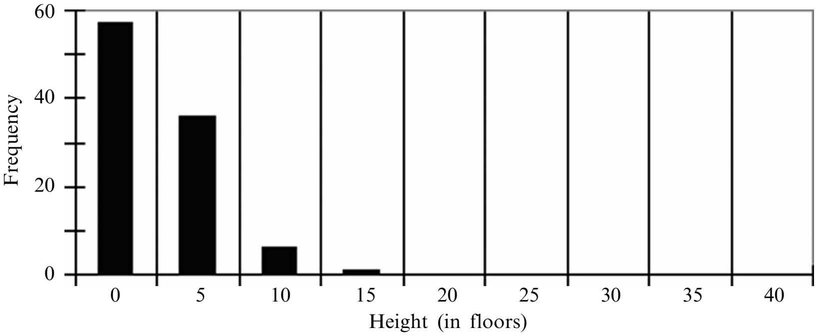

Figure 13. Distribution of height in the simulation model for class a pattern, where parameter values are: initial coverage = 40%, inertia = 50%, interaction = 2, and noise = 30%.

(3) It should be emphasized that every run of the model with the same value of parameters can lead to a different distribution of heights within the same class, but the general shape of distribution is the same in each class.

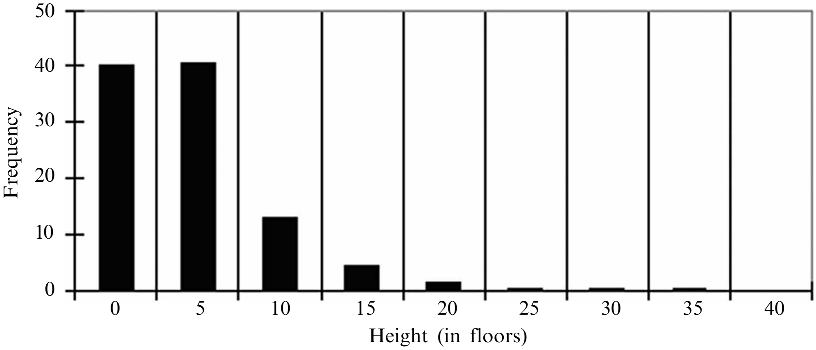

Figure 14. Distribution of height in the simulation model for class b pattern, where parameter values are: initial coverage = 60%, inertia = 100%, interaction = 5, and noise = 30%.

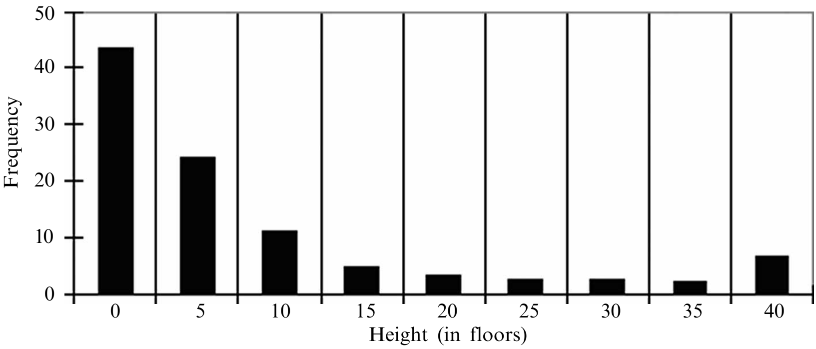

Figure 15. Distribution of height in the simulation for class c pattern, where parameter values are: initial coverage = 40%, inertia = 50%, interaction = 2, and noise = 60%.

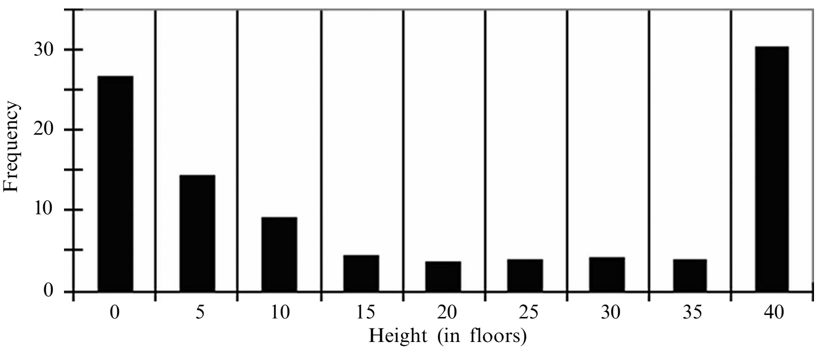

Figure 16. Distribution of height in the simulation model for class d pattern, where parameter values are: initial coverage = 40%, inertia = 50%, interaction = 2, and noise = 80%.

In this specific run the parameter values were initial coverage = 40%, inertia = 50%, interaction = 2, and noise = 30%.

Figure 14 presents the height distribution of buildings in class b. Just as in the case of class a, there is a large percentage of low heights (0 or 5), but in this class there are positive frequencies of high buildings (30 and 35 floors). The average height in this run is 4.438 floors.

Figures 15 – 17 present histograms of classes c, d, and e, respectively. The results in the upper classes (c, d, and e) are much different from lower classes (a and b). Class c,

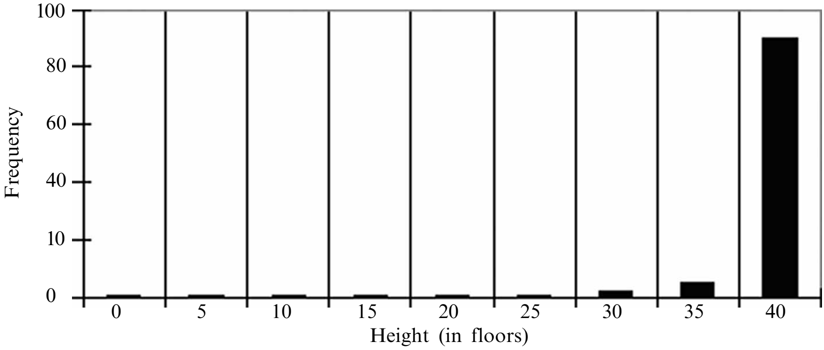

Figure 17. Distribution of height in the simulation model for class e pattern, where parameter values are: initial coverage = 40%, inertia = 50%, interaction = 2, and noise = 100%.

for example, presents a Pareto-like distribution of heights, but in classes d and, mainly, e the frequency of high buildings is much higher than the frequency of low buildings and the average height is much higher. Still, the basic difference between those classes is the considerable amount of low buildings in class d, whereas in class e their number is negligible. If the height limitation of H_{max} did not exist, almost 100% of the building's heights in class e could be above this artificial limit.

5 Examples of real cities

5.1 Clusters in Tel Aviv City

It is possible to identify real cities that represent counterparts to the above classification. As an illustrative example, Tel Aviv in the 2000s can be classified as a border class c city and this can be seen in figure 18 and in the map in figure 19. The map presents Tel Aviv and adjacent cities in 2003 (Ramat Gan, Givatym, and Bne Berak), where heights are classified to three distinct groups: low buildings (up to 10 m height), medium heights (between 10 m and 25 m), and high towers (more than 25 m). In this map we have circled possible arrangements of spatial clusters in Tel Aviv.

Figure 18. View of Tel Aviv, 2003, as an example of a border class c city.

Figure 19. Map of Tel Aviv and adjacent cities in 2003 (Ramat Gan, Givatym, and Bne Berak), where height is classified in three distinct groups: low buildings (up to 10 m height), medium-height buildings (between 10 m and 25 m), and high towers (more than 25 m). The possible cluster arrangements of towers in Tel Aviv are circled.[4]

From the map we can conclude the following points:

(1) Tel Aviv in 2003 can be classified as a nascent class c city. There are few spatial clusters of tall buildings. In the north and in the south there are clusters of residential towers. In the central region of Tel Aviv there are agglomerations of office towers and of residential towers, and near the coast there is a cluster of hotels. The clusters are not so connected and compact as the clusters in the simulation model, but their forms are generally similar to the spatial pattern of class c in the model. One of the reasons for this incompatibility between simulation results and reality is the absence of roads and highways in the simulation model.

(2) There is a huge cluster of medium buildings (the inner ring of Tel Aviv) and wide clusters of low buildings. The parameters of the CA model should be calibrated in future experiments in order to be adapted to these interesting spatial patterns, which seem to be an expansion of the five classes (a – e).

[4] The map was produced by a GIS database purchased from Survey of Israel, Agency for Geodesy, Cadastre, Mapping and Geographic Information.

Figure 20. View of Mexico City as an example of a class b city.

Figure 21. View of Toronto as an example of a class c city.

Figure 22. View of Chicago as an example of a class d city.

5.2 More examples of the different classes

A few examples of the different classes are presented in this section. Mexico City (see figure 20) can be considered as a class b city with separate tall buildings and without prominent agglomerations or spatial clusters.

Toronto (in figure 21) can be considered as a class c city, and Chicago (in figure 22) as a class d city. Class e is a hypothetical pattern and we cannot find cities in this classification in reality.

6 Conclusions and future research directions

The simulation model represents an attempt to depict the formation of 3D spatial order of cities. The results suggest that a relatively simple CA-type model can be used to describe the evolution of various cities. The model generates transitions through distinct spatial shapes. We have classified the shapes and indicated the means to produce these interesting morphologies. The CA dynamic model is based on simple and logical rules and can lead to powerful results that will help to describe complex systems in the future.

Our simulation model does not deal directly with economic variables like rent values,[5] but economic intuition is hidden in the current parameters. Rent values depend on the distribution of activities in the neighborhood and they are part of our interaction variable. Economies of scale, which are important economics forces are also represented by the inertia parameter. The noise parameter represents all the other influences not captured by inertia and interaction. It represents for example, ad hoc decisions of government and planners, and other factors. An interesting conclusion from this research is the fact that cities cannot develop only by the strong forces of inertia and interaction, but positive values of noise are also needed. An interesting challenge in future studies will be to explain and describe the ingredients of noise more carefully.

We are considering also the following improvements of the model:

(1) *Addition of destruction and fading processes*. It is noteworthy that the current version of the model does not include a possibility that a lower building will replace a higher building. Also, no removal of buildings takes place.

(2) *Addition of natural borders, green areas, and roads*. The geographic border of a city can include sea, a lake, or another kind of natural border. The simulation model does not include natural borders and green open areas, which are internal borders.

(3) *Spatial heterogeneity of parameters*. We have to consider the addition of different initial conditions at various locations in the city and variation of parameter values in different locations on the surface. Currently, the surface in the simulation model is homogeneous.

(4) *Calibration of model's parameters*. In order to make the model practical we have to calibrate time, area, and height units in the model according to a GIS database of real cities.

(5) *3D visualization*. The 3D model was developed on a 2D square base, and it is our intention to upgrade this model to a natural 3D environment. To this end we intend to program our model with the help of graphical tools, such as the new 3D StarLogo software version (StarLogo TNG, 2006), or other tools.

Acknowledgements. We wish to thank Erik Klopfer, Andrew Begel, and the Media Laboratory, MIT, Cambridge, for the use of StarLogo software and for their exceptional support and assistance.

[5] Economic and planning considerations of developers are the subject of another research project conducted in our research center.

References

Alonso W, 1964 *Location and Land Use* (Harvard University Press, Cambridge, MA)
Batty M, 1998, "Urban evolution on the desktop: simulation with the use of extended cellular automata" *Environment and Planning A* **30** 1943 – 1967
Batty M, 2005 *Cities and Complexity* (MIT Press, Cambridge MA)
Benguigui L, Czamanski D, Marinov M, Portugali Y, 2000, "When and where is a city fractal?" *Environment and Planning B: Planning and Design* **27** 507 – 519
Benguigui L, Czamanski D, Marinov M, 2001a, "The dynamics of urban morphology: the case of Petah Tikvah" *Environment and Planning B: Planning and Design* **28** 447 – 460
Benguigui L, Czamanski D, Marinov M, 2001b, "City growth as a leap-frogging process: an application to the Tel Aviv Metropolis" *Urban Studies* **38** 1819 – 1839
Benguigui L, Blumenfeld E, Czamanski D, 2006, "The dynamics of the Tel Aviv morphology" *Environment and Planning B: Planning and Design* **33** 269 – 284
Chen Q, Mynett A E, 2003, "Effect of cell size and configuration in cellular automata based prey-predator modeling" *Simulation Modelling Practice and Theory* **11** 609 – 625
Cheng J, Masser I, 2004, "Understanding spatial and temporal processes of urban growth: cellular automata modeling" *Environment and Planning B: Planning and Design* **31** 167 – 194
Couclelis H, 1997, "From cellular automata to urban models: new principles for model development and implementation" *Environment and Planning B: Planning and Design* **24** 165 – 174
Fujita M, 1982, "Spatial patterns of residential development" *Journal of Urban Economics* **12** 22 – 52
Fujita M, 1990 *Urban Economic Theory—Land Use and City Size* (Cambridge University Press, Cambridge)
Fujita M, Krugman P, Venables A J, 1999 *The Spatial Economy: Cities Regions and International Trade* (MIT Press, Cambridge, MA)
Garreau J, 1992 *Edge City: Life on the New Frontier* (Anchor Books, NY)
Glaeser E, Kahn M, 2001, "Decentralized employment and the transformation of the American city", WP 8117, National Bureau of Economic Research, New York
Henderson J V, 1974, "The sizes and types of cities" *American Economic Review* **64** 640 – 656
Hua W, Sprung D W L, 1998, "Three-dimensional simulation of quantum cellular automata and the zero-dimensional approximation" *Journal of Applied Physics* **84** 4000 – 4005
Hunt S M, Hamilton M A, Stewart P S, 2005, "A 3D model of antimicrobial action on biofilms" *Water Science and Technology* **52** 143 – 148
Kocabas V, Dragicevic S, 2006, "Assessing cellular automata model behaviour using a sensitivity analysis approach" *Computer, Environment and Urban Systems* **30** 921 – 953
Krakover S, 1985, "Spatio-temporal structure of population growth in urban regions: the cases of Tel-Aviv and Haifa, Israel" *Urban Studies* **22** 317 – 328
Krugman P, 1996 *The Self-organizing Economy* (Blackwell, Oxford)
McMillen D, Smith S, 2003, "The number of subcenters in large urban areas" *Journal of Urban Economics* **53** 321 – 338
Portugali J, 2000 *Self-organization and the City* (Springer, Berlin)
Semboloni F, 1997, "An urban and regional model based on cellular automata" *Environment and Planning B: Planning and Design* **24** 589 – 612
Semboloni F, 2000a, "The dynamic of an urban cellular automata in a 3-D spatial pattern", presented at XXI National Conference Aisre: Regional and Urban Growth in a Global Market, Palermo, http://fs.urba.arch.unifi.it/eng/ric/ca3d/index.html
Semboloni F, 2000b, "The growth of an urban cluster into a dynamic self-modifying spatial pattern" *Environment and Planning B: Planning and Design* **27** 549 – 564
Siregar P, Sinteff J P, Julen N, Le Beux P, 1998, "An interactive 3D anisotropic cellular automata model of the heart" *Computers and Biomedical Research* **31** 323 – 347
StarLogo, 2006, "StarLogo on the web", http://education.mit.edu/starlogo
StarLogo TNG, 2006, "Welcome to StarLogo TNG", http://education.mit.edu/starlogo-tng
White R, Engelen G, 1997, "Cellular automata as the basis of integrated dynamic regional modelling" *Environment and Planning B: Planning and Design* **24** 235 – 246
Wolfram S, 1986 *Theory and Application of Cellular Automata* (World Scientific, Singapore)